AGU100 ADVANCING EARTH AND SPACE SCIENCE

Geophysical Research Letters

RESEARCH LETTER
10.1029/2018GL078858

Key Points:
- An AFAI-biomass density model was established to estimate *Sargassum* biomass from reflectance
- *Sargassum* nutrients and pigments per *Sargassum* biomass were determined via field and laboratory measurements
- *Sargassum* biomass, nutrients, and pigments distributions in the Caribbean Sea and central West Atlantic were derived from MODIS

Supporting Information:
- Supporting Information S1

Correspondence to:
C. Hu,
huc@usf.edu

Citation:
Wang, M., Hu, C., Cannizzaro, J., English, D., Han, X., Naar, D., et al. (2018). Remote sensing of *Sargassum* biomass, nutrients, and pigments. *Geophysical Research Letters*, *45*, 12,359–12,367. https://doi.org/10.1029/2018GL078858

Received 27 MAY 2018
Accepted 19 JUL 2018
Accepted article online 25 JUL 2018
Published online 20 NOV 2018

Remote Sensing of *Sargassum* Biomass, Nutrients, and Pigments

Mengqiu Wang[1], Chuanmin Hu[1], Jennifer Cannizzaro[1], David English[1], Xingxing Han[1], David Naar[1], Brian Lapointe[2], Rachel Brewton[2], and Frank Hernandez[3]

[1]College of Marine Science, University of South Florida, Tampa, FL, USA, [2]Harbor Branch Oceanographic Institute, Florida Atlantic University, Fort Pierce, FL, USA, [3]Division of Coastal Sciences, University of Southern Mississippi, Ocean Springs, MS, USA

Abstract Field and laboratory experiments are designed to measure *Sargassum* biomass per area (density), surface reflectance, nutrient contents, and pigment concentrations. An alternative floating algae index-biomass density model is established to link the spectral reflectance to *Sargassum* biomass density, with a relative uncertainty of ~12%. Monthly mean integrated *Sargassum* biomass in the Caribbean Sea and central West Atlantic reached at least 4.4 million tons in July 2015. The average %C, %N, and %P per dry weight are 27.16, 1.06, and 0.10, respectively. The mean chlorophyll-a (Chl-a) concentration is ~0.05% of the dry weight. With these parameters, the amounts of nutrients and pigments can be estimated directly from remotely sensed *Sargassum* biomass. During bloom seasons, *Sargassum* carbon can account for ~18% of the total particulate organic carbon in the upper water column. This study provides the first quantitative assessment of the overall *Sargassum* biomass, nutrients, and pigment abundance from remote sensing observations, thus helping to quantify their ecological roles and facilitate management decisions.

1. Introduction

Pelagic *Sargassum* is a unique type of brown macroalgae that is mainly found in the Atlantic Ocean. It serves as a critical habitat and refuge to various marine organisms (Council, 2002; Doyle & Franks, 2015; Hu et al., 2016; Lapointe et al., 2014; Rooker et al., 2006; Witherington et al., 2012), and *Sargassum* sinking can potentially contribute to the carbon input to the deep-sea communities (Baker et al., 2017; Johnson & Richardson, 1977; Krause-Jensen & Duarte, 2016; Rowe & Staresinic, 1979). On the other hand, massive *Sargassum* beaching events can cause various environmental and economic problems in coastal areas of the Gulf of Mexico (GOM), Caribbean Sea (CS), and West Africa during bloom seasons (Franks et al., 2011; Hu et al., 2016; Schell et al., 2015; Webster & Linton, 2013). While large *Sargassum* aggregations in the Atlantic Ocean have been noted for centuries, a robust quantitative assessment of their total biomass is still lacking due to technical limitations. Early *Sargassum* biomass estimations mainly come from ship-based samplings using neuston tows (Butler et al., 1983; Butler & Stoner, 1984; Parr, 1939; Stoner, 1983). Parr measured the *Sargassum* biomass density in various locations in the Sargasso Sea and the tropical Atlantic and estimated a total biomass of 7–10 million tons in the Sargasso Sea (Parr, 1939). Stoner conducted another quantitative study and reported a major decrease of *Sargassum* biomass (Stoner, 1983), which was later attributed to the geographic variations within the Sargasso Sea and the sampling method (Butler & Stoner, 1984). More recently, the Sea Education Association collected neuston measurements in both Sargasso Sea and tropical Atlantic over the last 50 years and observed significant abundance changes especially in the tropical Atlantic (Schell et al., 2015; Siuda, 2011). However, given the significant seasonal and interannual variabilities of *Sargassum* abundance and distributions in the Intra-Americas Sea and North Atlantic (Wang & Hu, 2016, 2017), ship-based field measurements are likely biased for the basin-scale biomass estimation.

Because *Sargassum* has enhanced reflectance in the near-infrared spectral bands (this is often called *red-edge* reflectance), satellite and airborne instruments have been used to detect and quantify *Sargassum* (Dierssen et al., 2015; Gower & King, 2011; Hu, 2009; Hu et al., 2015, 2016). However, due to a lack of field or laboratory measurements, nearly all remote sensing studies have focused on the areal density or relative amount (Gower et al., 2013; Gower & King, 2011; Wang & Hu, 2016, 2017). On the other hand, knowledge of *Sargassum* biomass and its pigment compositions and nutrient contents, especially their distributions and temporal changes, is critical in quantifying its roles in biogeochemical cycling and ocean ecology (Baker et al., 2017; Lapointe, 1995; Lapointe et al., 2014; Rooker et al., 2006).

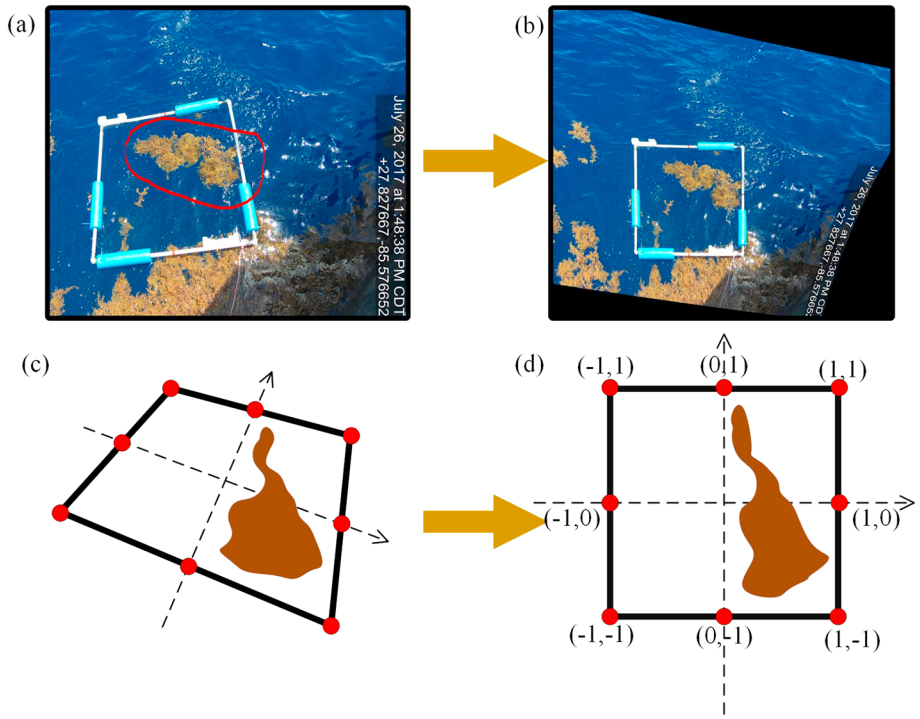

Figure 1. Quantification of *Sargassum* patch areal coverage using a 1-m^2 quadrat. (a) Original photo with the *Sargassum* patch inside the quadrat. The patch was collected immediately after the photo collection in order to determine its biomass; (b) rectified image based on the eight control points marked as red dots, as illustrated in (c) and (d).

Therefore, the objective here is to fill this knowledge gap by (1) developing a model to estimate *Sargassum* biomass density from reflectance; (2) determining *Sargassum* nutrient and pigment compositions and concentrations through field and laboratory measurements; and (3) mapping distributions of *Sargassum* biomass, nutrients, and pigments in the study region.

2. Materials and Methods

Sargassum samples were collected from eleven stations in the GOM and Florida Straits in April–July 2017 (Figure S1 in the supporting information). One station from Belize was also included in the analysis. Five types of *Sargassum* data were collected: (1) wet weight, (2) surface area, (3) surface reflectance, (4) pigment concentrations, and (5) nutrients of C, N, and P. Additional data of (1–3) collected in June 2018 in the GOM were also used.

2.1. *Sargassum* Biomass per Area

Sargassum biomass density was estimated by measuring the wet weight and areal coverage of an isolated patch (Figure 1) and repeating the measurements. A photo with both a 1-m^2 quadrat and the *Sargassum* patch was taken before collecting the *Sargassum* patch. The former was used to estimate the patch's area, while the latter was used to estimate the patch's weight. The sample was rinsed to remove vertebrates and invertebrates and drained for a few minutes to reduce the loose water, and then the wet weight was measured using a spring scale of 0.1-kg accuracy.

Because the digital photos typically have strong distortions, they were first rectified using the eight control points marked on the quadrat (Figure 1). Then the *Sargassum* areal density (D_S, kg/m^2) was calculated as

$$A_s = \frac{C_S}{C_Q} A_Q, \quad D_s = W_s / A_s \tag{1}$$

where A_S is the area (m^2) of the *Sargassum* patch, A_Q is the area of the quadrat (1 m^2), C_S is the pixel count of the patch, C_Q is the pixel count of the quadrat, and W_S is the wet weight (kg) of the patch.

2.2. Reflectance and AFAI Versus *Sargassum* Biomass Density

In separate bucket experiments, *Sargassum* reflectance was measured at different biomass densities in order to develop a model to estimate biomass density. The Spectral Evolution spectrometer covers the spectral range of 277–1,908 nm, with a field of view of 25° (Figure S2a).

Sargassum samples collected from the ocean were weighed using a spring scale with 1-g accuracy and put in a cooler. Twenty 25-g bags, six 70-g bags, and three 100-g bags of samples (29 total) were prepared. These samples were added one at a time to the black bucket filled with seawater forming 29 different densities, six of which are shown in Figure S2b. *Sargassum* biomass density was calculated as *Sargassum* weight divided by the bucket surface area ($\pi \times (0.47/2)^2$ m^2 = 0.17 m^2). Surface reflectance was measured at each of the 29 biomass densities approximately six times to establish a relationship between biomass density and reflectance (Figure S2c).

2.2.1. AFAI-Biomass Density Model

Following Wang and Hu (2016), alternative floating algae index (AFAI) was calculated using surface reflectance corresponding to Moderate Resolution Imaging Spectroradiometer (MODIS) bands, after applying the MODIS relative spectral response to the hyperspectral reflectance measured above:

$$AFAI = R_{748} - R_{667} - (R_{869} - R_{667})\frac{748 - 667}{869 - 667}, \quad (2)$$

where the numbers denote the MODIS bands in nanometers.

Each measured $R(\lambda)$ had a corresponding AFAI and biomass density, which were used to create a regression model. To apply the regression model to the satellite derived AFAI, the in situ AFAI was converted to MODIS AFAI using simulations under different atmospheric conditions. Two aerosol types were considered: maritime aerosol (90% humidity) and coastal aerosol (50% humidity). The aerosol optical thickness at 869 nm (τ_{869}) was tested from 0.04 to 0.44, where τ_{869} = 0.10 represented the mean condition for the study region (Wang & Hu, 2016). In situ AFAI measurements were then converted to MODIS AFAI, with the new AFAI-biomass density model applied to MODIS AFAI. In practice, because *Sargassum* percent coverage per pixel or per 0.5° grid was already derived (Wang & Hu, 2016) and each percent coverage corresponds to a MODIS AFAI value, such developed MODIS AFAI-biomass density model can be applied directly to the percent coverage maps.

2.2.2. Model Validation and Uncertainty Estimations

Direct model validation from satellite measurements is challenging due to the difficulty in linking the field-measured patch to the satellite-measured patch (Hu et al., 2017). There is further difficulty in conducting such measurements precisely within a MODIS 1 km × 1 km pixel area due to *Sargassum* patchiness. Reflectance data of 10 relatively dense and homogenous patches were collected while floating on the ocean surface, and their biomass densities were quantified with the method described in section 2.1. Additional black bucket (section 2.2) experiments were conducted to measure *Sargassum* reflectance to validate the model at various biomass density ranges.

2.3. *Sargassum* Pigments and Nutrient Concentrations

Sargassum samples were collected for tissue nutrient and pigment analyses. At each station, ~30 g *Sargassum* samples of both *Sargassum fluitans* (SF) and *Sargassum natans* (SN) were collected, rinsed briefly with DI water, and stored at −20 °C immediately after weighing and packing.

2.3.1. Sample Preparation

In the lab, frozen samples were freeze dried with the "Labconco freeze-dryer system" for 48–72 hr. For three stations in the Florida Straits and Belize, fresh samples were dried in a lab oven at 65°C, which may lead to small difference in the measured nutrient concentrations. The dried samples were ground into fine powders with a clean mortar and pestle. The corresponding dry weight for each *Sargassum* sample was measured to quantify the dry-to-wet weight ratio with a digital scale of 0.1-mg accuracy. The ground materials were transferred in plastic vials and stored at −20 °C until analyzed.

The ground samples were divided into three parts (subsamples) and analyzed as follows: two were used for pigment analyses (using spectrophotometry and high-performance liquid chromatography [HPLC]) and one for nutrient content measurements. For the first subsample, pigment extraction was conducted via vortexing ~0.1 g of the dried sample dissolved in 10 ml of 90% acetone for 30 s. The sample was then sonicated in Branson 5510 ultrasonic cleaner for 30 s. The mixture was stored in a −20 °C freezer for 24 hr to allow for sufficient pigment extraction. The absorption spectra of the pigment extracts were measured with a Perkin

Elmer Lambda 25 UV/Vis spectrophotometer. Concentrations of Chl-a and Chl-c were calculated using Jeffery and Humphrey (1975) equations. Figure S3 summarizes the main measurement processes, and Figure S4 shows the absorbance spectra collected. For the second subsample, pigment composition was analyzed by NASA-GSFC using HPLC with similar pigment extraction protocols (Hooker et al., 2005; Van Heukelem & Thomas, 2001). For the third subsample, the nutrient content analysis was conducted at the University of Georgia Analytical Chemistry Lab to determine tissue %C, %N, and %P per unit dried materials.

3. Results

3.1. Biomass Density of Pure *Sargassum* Patch

A total of 43 measurements were conducted from isolated *Sargassum* patches, of which 38 were from the GOM and five from the Florida Straits. The estimated biomass density is 3.54 ± 1.27 kg/m^2 in the GOM and 1.79 ± 0.55 kg/m^2 in the Florida Straits. For all samples, the average is 3.34 ± 1.34 kg/m^2, with a maximum of 6.74 kg/m^2 and a minimum of 1.26 kg/m^2.

3.2. *Sargassum* AFAI-Biomass Density Model and Its Uncertainties

Figure 2 shows the MODIS relative spectral response-weighed in situ AFAI against biomass density between 0.14 and 7.03 kg/m^2.

At low densities (<0.93 kg/m^2, AFAI < 0.04), AFAI increases linearly with density (R^2 = 0.98). At higher densities, a two-degree polynomial relationship was established (R^2 = 0.96). Thus, the AFAI-biomass density model was established as

$$\begin{aligned} y &= 23.34x && (0 < x \le 0.04) \\ y &= 104.88(x-0.04)^2 + 65.26(x-0.04) + 0.93 && (x > 0.04) \end{aligned} \tag{3}$$

where x is the AFAI value and y is the modeled *Sargassum* biomass density (kg/m^2).

The above model was based on in situ AFAI. Simulation results in Figure S5a showed tight relationship between MODIS AFAI and in situ AFAI. Under mean aerosol conditions (τ_{869} = 0.10), MODIS AFAI is ~75% of in situ AFAI (Figure S5b, R^2 = 1.00). Therefore, a multiplier of 1.33 was applied to convert MODIS AFAI to in situ AFAI before applying equation (3) to MODIS AFAI imagery (Figure S6).

The model's relative uncertainties were determined using independent measurements collected both in the bucket (blue squares in Figure 2) and in the ocean (gray triangles in Figure 2). The mean uncertainty was determined to be ~11%, and it appeared to be relatively consistent for both low and higher densities. Additional uncertainty comes from the variable atmospheric conditions. Under different conditions, the mean relative uncertainty in the MODIS AFAI was 1.2% with a maximum of 2.0%. Considering all uncertainty sources, the overall uncertainties in the modeled *Sargassum* biomass density should be <12% for a local patch.

3.3. MODIS-Derived *Sargassum* Biomass Density Distributions

Of all the *Sargassum*-containing pixels extracted from available MODIS images in 2015 covering the central West Atlantic (CWA) region, 99.5% have AFAI values lower than 0.0028 (i.e., within the linear range of 0–0.04 in the AFAI-biomass density model), corresponding to <6.23% *Sargassum* coverage within a pixel. For the monthly aggregated 0.5° grids, mean *Sargassum* percent coverage is usually <0.1% within a grid.

The monthly mean total biomass in the CS and CWA from 2011 to 2017, estimated from the MODIS-derived percent coverage (and its corresponding AFAI value; Wang & Hu, 2016) and the AFAI-biomass density model (equation (3)), are summarized in Table S1 and Figure 3 for the 0.5° grids. Note that these biomass estimations did not consider the dense *Sargassum* aggregations in the vertical direction, thus only representing lower-bound estimations. If the percent coverage were first converted to area coverage (m^2 in each 0.5° grid) and then converted to biomass using the field measured value of 3.34 kg/m^2 for pure *Sargassum* patches, the estimated biomass density would be 1.91 times the values in Figure 3b. According to the previous ship-based measurements (Butler & Stoner, 1984; Parr, 1939; Stoner, 1983), *Sargassum* biomass density in the GOM, CS, and North Atlantic typically ranged from 0.0 to 0.84 g/m^2 (Schell et al., 2015; Siuda, 2011). However, for the bloom conditions shown here, MODIS-derived biomass density could reach ~100 g/m^2 for the 1-km pixels

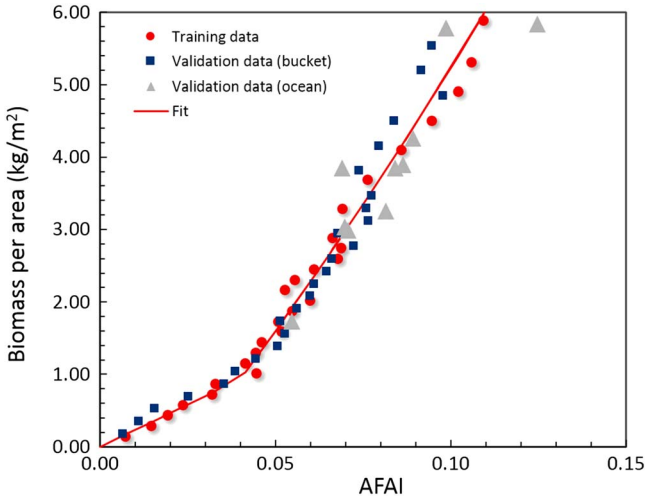

Figure 2. *Sargassum* biomass density (kg/m^2) versus in situ AFAI, determined from the bucket experiments (Figure S2) or measured in the ocean (Figure 1). The red line is the model fit (equation (3)) using training data (red circles). The blue squares represent validation data from other bucket experiments, while the gray triangles are from measurements in the ocean.

(Figure S6). Such dense patches at MODIS pixel scale would be unrealistic to sample in the field, therefore justifying the use of remote sensing to assess the large-scale *Sargassum* distributions.

The mean total *Sargassum* biomass in the CS and CWA for July 2015 is at least (i.e., lower bound) 4.4 million tons. This is within the same magnitude of the biomass estimation conducted by Parr (1939) for the Sargasso Sea (7–10 million tons). However, because the coarse MODIS pixels (1 km) cannot detect any *Sargassum* patch <2,000 m^2 (0.2% of a MODIS pixel, Wang & Hu, 2016) and because vertical aggregation of *Sargassum* cannot be remotely sensed, the MODIS-based estimates can only be used as a lower bound. Also note that if the central eastern Atlantic is included the total biomass would be much higher. On the other hand, even this lower bound is ~2.5 times of the daily maximum *Ulva prolifera* biomass in the Yellow Sea in 2015 (Hu et al., 2017), indicating the unprecedented scale and intensity of the *Sargassum* bloom.

3.4. Major Pigment and Nutrient Concentrations of *Sargassum*

The *Sargassum* nutrient contents are summarized in Table 1. Most stations here are from neritic waters (within 70 km offshore, see Figure S1). There are only three stations that are more oceanic (200 - 250 km offshore), but their nutrient compositions did not show a large difference from neritic stations. In this study, neritic stations are within 70 km offshore while oceanic stations are >70 km offshore. This definition of the oceanic station is very different from that used in Lapointe (1995) and Lapointe et al. (2014, 2015), which defines the stations in the Sargasso Sea as the oceanic stations. Therefore, the results

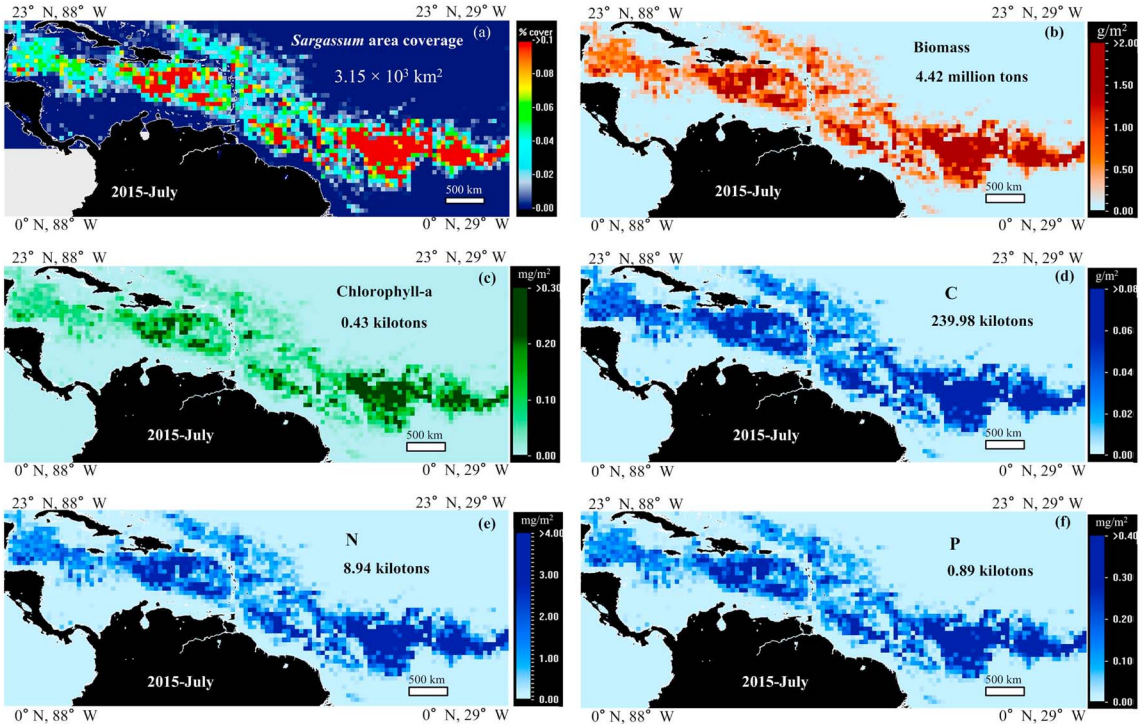

Figure 3. Monthly mean *Sargassum* areal coverage (%), biomass density, Chl-a, C, N, and P in each 0.5° grid in the Caribbean Sea and central West Atlantic in July 2015. Based on the mean concentrations measured in this study, the biomass, nutrients, and pigments in (b–f) were derived from the *Sargassum* percent coverage (and the corresponding alternative floating algae index) in (a) using equation (3). The total integrated *Sargassum* areal coverage, wet biomass, nutrients, and pigments over the bloom areas (density > 0.0%) are annotated in each panel.

Table 1
Sargassum Nutrient Contents and Ratios per Unit Dry Weight and Major Pigment Concentrations Measured by HPLC (unit: ng mg d.w.$^{-1}$)

		Sample size	%C	%N	%P	C:N	C:P	N:P	Chl-a	Chl-c
Overall mean	SF	201	26.49 ± 1.79	1.11 ± 0.29	0.11 ± 0.03	30.80 ± 15.43	694.94 ± 275.82	23.68 ± 7.32	439.05 ± 70.48	36.68 ± 6.71
	SN	87	28.35 ± 2.45	0.95 ± 0.30	0.09 ± 0.03	38.81 ± 13.05	926.24 ± 339.24	24.24 ± 5.47	537.93 ± 54.82	42.41 ± 5.34
	Combined	288	27.16 ± 2.23	1.06 ± 0.31	0.10 ± 0.03	33.66 ± 15.08	777.55 ± 318.83	23.88 ± 6.70	485.20 ± 101.28	39.36 ± 6.69
Neritic	SF	153	26.94 ± 1.82	1.07 ± 0.30	0.11 ± 0.04	32.99 ± 17.39	727.39 ± 316.59	23.11 ± 8.11	NAN	NAN
	SN	66	29.24 ± 2.02	0.88 ± 0.28	0.08 ± 0.02	42.47 ± 12.32	983.90 ± 310.12	23.74 ± 5.62	NAN	NAN
	Combined	219	27.76 ± 2.19	1.00 ± 0.31	0.10 ± 0.03	36.37 ± 16.35	818.72 ± 336.26	23.33 ± 7.30	NAN	NAN
Oceanic	SF	48	25.10 ± 5.45	1.23 ± 0.24	0.11 ± 0.01	25.10 ± 5.45	610.98 ± 68.40	25.15 ± 5.45	NAN	NAN
	SN	21	29.41 ± 10.05	1.13 ± 0.31	0.10 ± 0.04	29.41 ± 10.05	777.96 ± 376.76	25.53 ± 5.05	NAN	NAN
	Combined	69	25.59 ± 7.60	1.19 ± 0.26	0.11 ± 0.03	26.65 ± 7.60	670.92 ± 241.04	25.29 ± 4.62	NAN	NAN

Note. SF = *Sargassum fluitans*; SN = *Sargassum natans*; Combined = *Sargassum* whole samples containing both SN and SF. NAN means not calculated.

and conclusions from those studies regarding the oceanic water cannot be compared with this study. Overall, nutrient compositions are relatively stable for all samples. The mean %C, %N, and %P per dry weight (d.w.) are 27.16, 1.06, and 0.10, respectively.

Tables 1 and S2 summarize Chl-a and Chl-c pigment concentrations determined from both spectrophotometric and HPLC measurements. The mean Chl-a concentration (HPLC) is 485.20 ± 101.28 ng mg d.w.$^{-1}$, representing ~0.05% of the total dry biomass. The Chl-a:Chl-c ratio is 0.08 ± 0.01 from all HPLC measurements. Overall, pigment compositions are stable for both species. The two major light-harvesting pigments are Chl-a and fucoxanthin, accounting for ~60% and 20% of the total major pigment contents (Table S3). All other pigments are an order of magnitude lower. The results from the spectrophotometric measurements are close to those from the HPLC measurements.

The HPLC-measured mean concentrations from all samples were used to derive pigment concentrations from biomass density and to compare with those values reported by Schofield et al. (1998). The concentrations from this study are consistently higher for all major pigments for both SF and SN (Table S3). It is unclear whether this is due to seasonal variations, measurement protocols, or real changes during the 20-year period. However, the relative fractions of the major pigments are consistent from both studies (Figure S7).

4. Discussions

4.1. *Sargassum* Pigments

Sargassum reflectance properties are determined primarily from pigment composition: Each pigment has its own absorption characteristics. For example, the reflectance troughs at 630 and 670 nm are caused by the strong absorption by Chl-c and Chl-a, respectively (Bricaud et al., 2004). The low Chl-c:Chl-a ratio (0.08) can explain the different magnitudes of these reflectance troughs. Likewise, the low reflectance between 400 and 500 nm (the reason why *Sargassum* does not have any blueish-greenish colors) is caused by Chl-a absorption around 440 nm and fucoxanthin absorption around 500 nm (Bricaud et al., 2004). The low reflectance in the green wavelengths is expected and helps discriminate *Sargassum* from *Trichodesmium*. This cyanobacteria (also called blue-green algae) is also abundant in the Atlantic Ocean (Hu et al., 2015) and similar to *Sargassum* in that it also shows red-edge reflectance when algae cells or colonies form surface scums. These reflectance characteristics, associated with the major pigment absorptions, might eventually be used to develop algorithms to assess *Sargassum* life stages and physiological states.

4.2. *Sargassum* Carbon

As shown in Figure 3d, the massive *Sargassum* bloom in the CS and CWA contained large amounts of carbon that have not been considered in any carbon cycle models. Is this a negligible component when compared to the traditional water-column phytoplankton carbon (i.e., particulate organic carbon or POC)? Or is it a vital component required to improve carbon cycle models? As *Sargassum* lives mostly in nutrient-poor open-ocean waters with low water-column Chl-a concentrations, POC from a layer 50 m deep of 0.1-mg/m^3 Chl-

a concentration was used to compare with *Sargassum* carbon. The former is equivalent to an integrated water column Chl-a density of 5.0 mg/m^2. Assuming the mean C:Chl-a ratio of 74 (g:g) in the Atlantic Ocean (Wang et al., 2013), the water column POC is 0.37 g/m^2. In comparison, for waters with *Sargassum* biomass density >0.0 g/m^2 in July 2015 (an area of 7.23×10^6 km^2), *Sargassum* Chl-a, wet biomass, and carbon were estimated to be 0.06 mg/m^2, 0.61 g/m^2, and 0.03 g/m^2, respectively. Although these numbers are lower than those of the water-column phytoplankton, the *Sargassum* contributions to total carbon (~9%) should not be neglected. On the other hand, for the entire study region (1.16×10^7 km^2), because some waters have 0.0 g/m^2 *Sargassum*, the mean *Sargassum* Chl-a, biomass, and carbon in July 2015 are reduced to 0.04 mg/m^2, 0.38 g/m^2, and 0.02 g/m^2, respectively. This still indicates that *Sargassum* carbon can represent a significant component (~6%).

In addition to MODIS-observed *Sargassum*, there may also exist many small-scale *Sargassum* features that are undetectable by MODIS. Given the detection limit of 0.2% coverage within MODIS 1-km pixels (Wang & Hu, 2016), the lowest biomass density measured from a MODIS pixel is 2.80 g/m^2, higher than most field-measured values. Given the fact that field measurements are mostly through neuston nets for small *Sargassum* mats or clumps, field collected *Sargassum* densities may represent the undetected proportion. Adding the field-measured biomass density of 0.84 g/m^2 (during November 2014 to May 2015; Schell et al., 2015) to MODIS measurements (0.38 g/m^2; note that this value appears lower than the pixel-level detection limit, but it is a result of monthly averaging), the mean Chl-a, biomass, and carbon are 0.12 mg/m^2, 1.22 g/m^2, and 0.07 g/m^2 in the entire study regions, respectively. Thus, the total *Sargassum* carbon can account for ~18% of the phytoplankton carbon over the entire study region during the peak months. By failing to account for this much carbon, it is clear that current carbon cycle models could be improved by including total *Sargassum* carbon.

4.3. *Sargassum* Nutrient Limitations

Compared to the Redfield Ratio (106:16:1; Redfield, 1934), the *Sargassum* C:N:P data suggest a strong nutrient limitation of both N and P. According to the neritic baseline from Lapointe et al. (2014, 2015), %N, N:P, C:N, and C:P of SF are about 1, 10, 27, and 268, respectively. Compared to historical baselines, the results from this study did not show a significant increase of %N for SF, which dominated the sample collections. However, the mean N:P (23.11) and C:P (727.39) of SF are much higher than the neritic baseline for all cases, suggesting a consistently stronger P-limitation than historical samples. The %N and %P of SN are slightly lower than those of SF, but their %C is higher. Our results indicate that the recent *Sargassum* blooms may be enhanced by long-term nutrient enrichment. This is especially relevant given the global N-enrichment during the past decades (Galloway et al., 2008; Rockström et al., 2009). As riverine N-loading is expected to increase by 19% before 2100 due to changes in precipitation along (Sinha et al., 2017), it will be important to better understand the relationship between *Sargassum* blooms and nutrient loading.

4.4. *Sargassum* Sedimentation on the Deep-Sea Floor

Carbon and nutrients in *Sargassum* also impact the deep-sea ecosystems once the algae die and sink to the ocean bottom. In fact, connection of *Sargassum* to the deep-sea communities has been confirmed in field surveys where sinking *Sargassum* was observed on the ocean floor (Johnson & Richardson, 1977; Rowe & Staresinic, 1979). These observations suggest that macroalgae may play an important role in carbon transport to the deep-sea fauna (Krause-Jensen & Duarte, 2016). Considering the enormous blooms in the CS and CWA in recent years, massive carbon sedimentation may have already provided significant carbon input, thus potentially affecting the deep-sea fauna distribution patterns (Baker et al., 2017). Additional support for carbon sedimentation comes from sediment core studies near the Deepwater Horizon Wellhead MC252 following the April 2010 oil blowout in the GOM. The cores showed elevated accumulations of carbon-rich sediments likely resulting from a major marine snow event associated with hydrocarbon-induced microbial blooms (Brooks et al., 2015; Paul et al., 2013) and sediment porewater genotoxicity (Paul et al., 2013). Although the initiations of these sedimentation events are different, the resulting major carbon sedimentary accumulation should be similar. In the end, once field data are available to link *Sargassum* deposition and remotely sensed biomass, the basin-scale biomass estimation from this study may help quantify the amount of carbon deposition and infer its potential impact.

Acknowledgments
Financial support has been provided by the U.S. NASA Ocean Biology and Biogeochemistry Program (NNX14AL98G and NNX16AR74G) and Ecological Forecast Program (NNX17AE57G), NOAA RESTORE Science Program (NA17NOS4510099), and by a William and Elsie Knight Endowed Fellowship. We thank NASA for providing MODIS data for this analysis. All *Sargassum* relevant imagery data products are available through the *Sargassum* Watch System (SaWS, http://optics.marine.usf.edu/projects/saws.html). We thank Mr. Brock Murch for his various editorial comments and Mr. Brian Jones for his help in collecting *Sargassum* samples.

References

Baker, P., Minzlaff, U., Schoenle, A., Schwabe, E., Hohlfeld, M., Jeuck, A., et al. (2017). Potential contribution of surface-dwelling Sargassum algae to deep-sea ecosystems in the southern North Atlantic. *Deep Sea Research Part II: Topical Studies in Oceanography*, *148*, 21–34.

Bricaud, A., Claustre, H., Ras, J., & Oubelkheir, K. (2004). Natural variability of phytoplanktonic absorption in oceanic waters: Influence of the size structure of algal populations. *Journal of Geophysical Research*, *109*, C11010. https://doi.org/10.1029/2004JC002419

Brooks, G. R., Larson, R. A., Schwing, P. T., Romero, I., Moore, C., Reichart, G.-J., et al. (2015). Sedimentation pulse in the NE Gulf of Mexico following the 2010 DWH blowout. *PLoS One*, *10*(7), e0132341. https://doi.org/10.1371/journal.pone.0132341

Butler, J. N., Morris, B. F., Cadwallader, J., & Stoner, A. W. (1983). Studies of Sargassum and the Sargassum community, Bermuda Biological Station, Special Publication (Vol. 22, pp. 1–85).

Butler, J. N., & Stoner, A. W. (1984). Pelagic Sargassum: Has its biomass changed in the last 50 years? *Deep Sea Research Part A. Oceanographic Research Papers*, *31*(10), 1259–1264. https://doi.org/10.1016/0198-0149(84)90061-X

Council, S. A. F. (2002). Fishery management plan for pelagic Sargassum habitat of the South Atlantic region, (Online) http://www.safmc.net/Portals/6/Library/FMP/Sargassum/SargFMP.pdf

Dierssen, H., Chlus, A., & Russell, B. (2015). Hyperspectral discrimination of floating mats of seagrass wrack and the macroalgae Sargassum in coastal waters of Greater Florida Bay using airborne remote sensing. *Remote Sensing of Environment*, *167*, 247–258. https://doi.org/10.1016/j.rse.2015.01.027

Doyle, E., & Franks, J. (2015). Sargassum fact sheet, Gulf and Caribbean Fisheries Institute.

Franks, J., Johnson, D., Ko, D., Sanchez-Rubio, G., Hendon, J., & Lay, M. (2011). Unprecedented influx of pelagic Sargassum along Caribbean Island coastlines during summer 2011, *Proceedings of the 64th Gulf and Caribbean Fisheries Institute*, Puerto Morelos, 5.

Galloway, J. N., Townsend, A. R., Erisman, J. W., Bekunda, M., Cai, Z., Freney, J. R., et al. (2008). Transformation of the nitrogen cycle: Recent trends, questions, and potential solutions. *Science*, *320*(5878), 889–892. https://doi.org/10.1126/science.1136674

Gower, J., Young, E., & King, S. (2013). Satellite images suggest a new Sargassum source region in 2011. *Remote Sensing Letters*, *4*(8), 764–773. https://doi.org/10.1080/2150704X.2013.796433

Gower, J. F., & King, S. A. (2011). Distribution of floating Sargassum in the Gulf of Mexico and the Atlantic Ocean mapped using MERIS. *International Journal of Remote Sensing*, *32*(7), 1917–1929. https://doi.org/10.1080/01431161003639660

Hooker, S. B., Van Heukelem, L., Thomas, C. S., Claustre, H., Ras, J., Barlow, R., et al. (2005). The second SeaWiFS HPLC analysis round-robin experiment (SeaHARRE-2), *NASA Tech*. Memo, 212785, 124.

Hu, C. (2009). A novel ocean color index to detect floating algae in the global oceans. *Remote Sensing of Environment*, *113*(10), 2118–2129. https://doi.org/10.1016/j.rse.2009.05.012

Hu, C., Feng, L., Hardy, R. F., & Hochberg, E. J. (2015). Spectral and spatial requirements of remote measurements of pelagic Sargassum macroalgae. *Remote Sensing of Environment*, *167*, 229–246. https://doi.org/10.1016/j.rse.2015.05.022

Hu, C., Murch, B., Barnes, B., Wang, M., Maréchal, J., Franks, J., et al. (2016). Sargassum watch warns of incoming seaweed. *Eos Transactions American Geophysical Union*, *97*. https://doi.org/10.1029/2016EO058355

Hu, L., Hu, C., & He, M.-X. (2017). Remote estimation of biomass of *Ulva prolifera* macroalgae in the Yellow Sea. *Remote Sensing of Environment*, *192*, 217–227. https://doi.org/10.1016/j.rse.2017.01.037

Jeffrey, S. t., & Humphrey, G. (1975). New spectrophotometric equations for determining chlorophylls a, b, c1 and c2 in higher plants, algae and natural phytoplankton. *Biochemie und Physiologie der Pflanzen*, *167*(2), 191–194. https://doi.org/10.1016/S0015-3796(17)30778-3

Johnson, D. L., & Richardson, P. L. (1977). On the wind-induced sinking of Sargassum. *Journal of Experimental Marine Biology and Ecology*, *28*(3), 255–267. https://doi.org/10.1016/0022-0981(77)90095-8

Krause-Jensen, D., & Duarte, C. M. (2016). Substantial role of macroalgae in marine carbon sequestration. *Nature Geoscience*, *9*(10), 737–742. https://doi.org/10.1038/ngeo2790

Lapointe, B., Herren, L. W., Feibel, A., & Hu, C. (2015). Evidence of nitrogen-fueled blooms of pelagic Sargassum in the Gulf of Mexico, *Annual conference of the Gulf and Caribbean Fisheries Institute*.

Lapointe, B. E. (1995). A comparison of nutrient-limited productivity in Sargassum natans from neritic vs. oceanic waters of the western North Atlantic Ocean. *Limnology and Oceanography*, *40*(3), 625–633. https://doi.org/10.4319/lo.1995.40.3.0625

Lapointe, B. E., West, L. E., Sutton, T. T., & Hu, C. (2014). Ryther revisited: Nutrient excretions by fishes enhance productivity of pelagic Sargassum in the western North Atlantic Ocean. *Journal of Experimental Marine Biology and Ecology*, *458*, 46–56. https://doi.org/10.1016/j.jembe.2014.05.002

Parr, A. E. (1939). Quantitative observations on the pelagic Sargassum vegetation of the western North Atlantic. *Bulletin of the Bingham Oceanographic Collection*, *6*, 1–94.

Paul, J. H., Hollander, D., Coble, P., Daly, K. L., Murasko, S., English, D., et al. (2013). Toxicity and mutagenicity of Gulf of Mexico waters during and after the Deepwater Horizon oil spill. *Environmental Science & Technology*, *47*(17), 9651–9659. https://doi.org/10.1021/es401761h

Redfield, A. C. (1934). *On the proportions of organic derivatives in sea water and their relation to the composition of plankton*, James Johnstone memorial volume (pp. 176–192). Liverpool: University Press of Liverpool.

Rockström, J., Steffen, W., Noone, K., Persson, Å., Chapin, F. S. III, Lambin, E. F., et al. (2009). A safe operating space for humanity. *Nature*, *461*(7263), 472.

Rooker, J. R., Turner, J. P., & Holt, S. A. (2006). Trophic ecology of Sargassum-associated fishes in the Gulf of Mexico determined from stable isotopes and fatty acids. *Marine Ecology Progress Series*, *313*, 249–259. https://doi.org/10.3354/meps313249

Rowe, G. T., & Staresinic, N. (1979). Sources of organic matter to the deep-sea benthos, Ambio Special Report, 19-23.

Schell, J. M., Goodwin, D. S., & Siuda, A. N. (2015). Recent Sargassum inundation events in the Caribbean: Shipboard observations reveal dominance of a previously rare form. *Oceanography*, *28*(3), 8–10. https://doi.org/10.5670/oceanog.2015.70

Schofield, O., Evens, T. J., & Millie, D. F. (1998). Photosystem II quantum yields and xanthophyll-cycle pigments of the macroalga Sargassum natans (phaeophyceae): Responses under natural sunlight. *Journal of Phycology*, *34*(1), 104–112. https://doi.org/10.1046/j.1529-8817.1998.340104.x

Sinha, E., Michalak, A. M., & Balaji, V. (2017). Eutrophication will increase during the 21st century as a result of precipitation changes. *Science*, *357*(6349), 405–408. https://doi.org/10.1126/science.aan2409

Siuda, A. N. (2011). Summary of sea education association long-term Sargasso sea surface net data, Edited, *Sargasso Sea Alliance Science Report Series*.

Stoner, A. W. (1983). Pelagic Sargassum: Evidence for a major decrease in biomass. *Deep Sea Research Part A. Oceanographic Research Papers*, *30*(4), 469–474. https://doi.org/10.1016/0198-0149(83)90079-1

Van Heukelem, L., & Thomas, C. S. (2001). Computer-assisted high-performance liquid chromatography method development with applications to the isolation and analysis of phytoplankton pigments. *Journal of Chromatography A*, *910*(1), 31–49. https://doi.org/10.1016/S0378-4347(00)00603-4

Wang, M., & Hu, C. (2016). Mapping and quantifying Sargassum distribution and coverage in the central West Atlantic using MODIS observations. *Remote Sensing of Environment*, *183*, 350–367. https://doi.org/10.1016/j.rse.2016.04.019

Wang, M., & Hu, C. (2017). Predicting Sargassum blooms in the Caribbean Sea from MODIS observations. *Geophysical Research Letters*, *44*, 3265–3273. https://doi.org/10.1002/2017GL072932

Wang, X., Murtugudde, R., Hackert, E., & Marañón, E. (2013). Phytoplankton carbon and chlorophyll distributions in the equatorial Pacific and Atlantic: A basin-scale comparative study. *Journal of Marine Systems*, *109*, 138–148.

Webster, R. K., & Linton, T. (2013). Development and implementation of Sargassum early advisory system (SEAS). *Shore & Beach*, *81*(3), 1.

Witherington, B., Hirama, S., & Hardy, R. (2012). Young sea turtles of the pelagic Sargassum-dominated drift community: Habitat use, population density, and threats. *Marine Ecology Progress Series*, *463*, 1–22. https://doi.org/10.3354/meps09970